Available online at www.sciencedirect.com
SCIENCE DIRECT®
Polymer 44 (2003) 4625–4634
polymer
www.elsevier.com/locate/polymer

# Preparation and characterization of new melt compounded copolyamide nanocomposites

L. Incarnato[a,*], P. Scarfato[a], G.M. Russo[a], L. Di Maio[a], P. Iannelli[a], D. Acierno[b]

[a]*Department of Chemical and Food Engineering, University of Salerno, Via Ponte don Melillo, 84084 Fisciano (SA), Italy*
[b]*Department of Materials and Production Engineering, University of Naples 'Federico II', P.le Tecchio 80, 80125 Napoli, Italy*

Received 20 March 2003; received in revised form 10 April 2003; accepted 30 April 2003

**Abstract**

In this work new copolyamide-layered silicate nanocomposites were prepared by melt compounding using a commercial polyamide 6-based copolymer, with a partially aromatic structure, as thermoplastic matrix. This copolyamide, having a lower melting point and improved mechanical and barrier properties respect to the homopolymer, appears an interesting material for producing nanocomposite packaging films. Hybrids with different organoclay loadings were produced by a twin-screw extruder using different extrusion rates, in order to point out the effects of both processing conditions and hybrid composition on morphology (silicate dispersion and exfoliation, orientation, matrix crystallinity) of nanocomposites. All melt-intercalated samples were submitted to structural (TEM and XRD), thermal and dynamic mechanical measurements. The performed analyses have evidenced that all hybrids exhibit mixed intercalated/exfoliated morphology and that the extent of exfoliation increases with both clay amount and extrusion rate used. Moreover, it was pointed out that the silicate nano-scale dispersion significantly affects the crystalline morphology of copolyamide matrix, stabilizing the γ-crystal phase, and the dynamic mechanical response of the hybrids, whose storage and loss moduli values result sensibly higher than those corresponding to the neat matrix.


*Keywords:* Nanocomposites; Melt compounding; Copolyamide

## 1. Introduction

Polyamides are large volume plastics widely used for structural and packaging applications. Their market spread is continuously growing due to their properties such as chemical and mechanical resistance, good barrier properties to gases, clarity, printability, etc. The ultimate properties of end products are, of course, heavily dependent on the chemical structure of polyamide and on the process used to produce the manufactured articles [1–3] and can be further increased using nanoparticles as additives to enhance the polymer performance. At this regard, over last decade scientific research has paid great attention to polyamide/layered silicate nanocomposites because, compared to the unmodified resin, these systems provide enhanced performance properties such as improved tensile strength and moduli, decreased thermal expansion coefficient, decreased gas permeability, increased swelling resistance, enhanced ion conductivity, reduced flammability, etc [4–9]. In particular, a growing interest is devoted towards polyamide-based nanocomposites prepared by melt compounding: this production technique, in fact, seems to be very attractive from a technological and a commercial point of view for its versatility and compatibility with the conventional polymer manufacturing processes [5,10,11]. Nevertheless, polymer/layered silicate nanocomposites (PLSNs) have not still achieved a wide market spread, due to the difficulty in conveniently tuning materials and processing parameters to control the developed morphology (clay dispersion and exfoliation degree, matrix crystallinity, orientation) and then the performance enhancement of nanocomposite systems. Consequently, the understanding of processing-morphology-property relationships is indispensable to optimize and predetermine the PLSNs performances and could give rise to new market opportunities for nanocomposite materials. The need to control the nano-scale structure of melt compounded PLSNs is particularly pressing for semicrystalline polymers such as polyamides. The final properties will depend, in fact, not only on

* Corresponding author. Tel.: +39-89-964-144; fax: +39-89-964-057.
*E-mail address:* lincarnato@unisa.it (L. Incarnato).

0032-3861/03/$ - see front matter © 2003 Elsevier Science Ltd. All rights reserved.
doi:10.1016/S0032-3861(03)00360-4

distribution of layered silicate but also on the influence of polymer–silicate interactions on polymer crystallization and crystallite morphology.

Many works are reported in literature on the effects of layered silicate nanoscale dispersion in melt compounded polyamide matrixes [4,10–17]. From these studies the following important points appear to emerge:

— the degree of exfoliation realized in the hybrids strictly depends on matrix viscosity and polymer-clay affinity;
— the processing temperatures and the organoclay used have to be opportunely selected so to avoid thermal degradation of the organoclay;
— an optimum balance between residence time and level of shear in the extruder is required to facilitate the exfoliation and the dispersion of layered silicate.

In this field, we are conducting a study on the possibility to improve processability and properties of melt compounded polyamide-silicate nanocomposites using a copolyamide resin as matrix. The selected copolyamide was a commercial resin (traded by Caffaro SpA, Italy, as ADS 40T), already used in our previous study [18] conducted on several neat polyamide 6-based copolymers. ADS 40T resin contains random the comonomer 1,1′,3-trimethylcyclohexil-3-methylamine-5-isophtalamide at 5 wt%; its incorporation into polyamide 6 homopolymer chain assures a depression of the melting point [19], what allowed to use lower extrusion temperatures respect to the homopolymer. Moreover, our studies have shown that ADS films exhibit also increased mechanical and barrier performance. Finally, the rigid, partially aromatic nature of this comonomer could stabilize extended conformational arrangements of the macromolecules making easier the polymer intercalation in the organoclay galleries. From these considerations, the ADS 40T copolymer appears an interesting material for producing nanocomposites packaging films. In order to investigate the effect of both processing conditions and hybrid composition on the morphology and properties of these nanocomposite systems, ADS 40T was melt compounded with three silicate loadings of a commercial organically modified montmorillonite, using different screw speeds. The produced samples were submitted to structural, thermal and dynamic mechanical analyses.

## 2. Experimental

### 2.1. Materials

Raw materials used for the preparation of copolyamide-clay nanocomposites were the Cloisite 30B (supplied by Southern Clay Products, Inc.), a layered sodium montmorillonite organically modified by *N*,methyl-*N*,tallow-*N*,*N*′,2-hydroxyethyl-ammoniumchloride (90 meq/100 g clay), having interlayer basal spacing $d_{001} = 18.5$ Å, and a copolyamide matrix (traded as ADS 40T, IV = 2.9 dl/g), supplied by Caffaro SpA (Italy), derived by random polymerization of ε-caprolactam in presence of the comonomer 1,1′,3-trimethylcicloesil-3,metilamine-5,isoftalamide at 5 wt%. The molecular structure of ADS copolyamide is shown in Fig. 1.

### 2.2. Melt processing

The polyamide-layered silicate nanocomposites were prepared by melt compounding using an Haake twin-screw extruder having counter-rotating intermeshing cone-shaped screws with $L = 300$ mm. The screw design allows to have varying degrees of mixing along the length of the screws. A temperature profile of 265–260–255–245 °C from hopper to die was imposed and a rectangular die (1 × 40 mm) was used. Prior the processing, the materials were dried in a vacuum oven at 87 °C for 18 h obtaining a moisture level below 0.2 wt% in order to avoid bubble formation and polymer degradation during processing [20]. Nanocomposite ribbons at different organoclay content (3, 6 and 9 wt%) were extruded at three screw speeds: 50, 80 and 100 rpm, corresponding to average residence times in the extruder of about 3.5, 3.0 and 2.5 min, respectively. The processing conditions and sample nomenclature used for the discussion of results are reported in Table 1.

### 2.3. Characterization

The effective level of silicate into each extruded sample was determined drying each sample at 100 °C for 18 h under vacuum and weighting it before placing in a furnace at 900 °C for 45 min in air. The amount of residue was measured and corrected for the loss of organic percent in Cloisite 30B experimentally verified. Each determination was replaced on five specimens to obtain statistical silicate loading values.

Transmission electron microscopy (TEM) analysis was conducted using a Philips EM 208 with different magnification levels. The images were captured on sections located normal and parallel to the extrusion direction, prepared by microtoming of ultra-thin specimens with a Leica Utracut UCT microtome.

X-ray diffraction (XRD) experiments were performed with a Philips 1830 Powder diffractometer, using a Ni-filtered CuKα radiation. A flat camera with a sample-to-film distance of 140 mm was used to collect the data. The Fujifilm MS 2025 imaging plate and the Fuji Bio-imaging

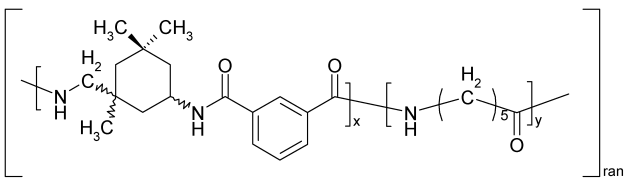


Fig. 1. Molecular structure of ADS copolyamide.

Table 1
Processing conditions and sample nomenclature

| Nominal wt%, Cloisite 30B | Screw speed (rpm) | ADS40T-based hybrids |
|---|---|---|
| 3 | 50 | 3ADS50 |
| | 80 | 3ADS80 |
| | 100 | 3ADS100 |
| 6 | 50 | 6ADS50 |
| | 80 | 6ADS80 |
| | 100 | 6ADS100 |
| 9 | 50 | 9ADS50 |
| | 80 | 9ADS80 |
| | 100 | 9ADS100 |

Analyzer System (mod. BAS-1800) were used for digitizing the diffraction patterns.

The non-isothermal analyses of the samples were carried out using a Mettler Differential Scanning Calorimeter mod. DSC30 on samples as extruded and on samples annealed under vacuum oven at 200 °C for 1 and 5 h, to investigate the effect of an annealing treatment on the thermal response of nanocomposite samples. A thermal cycle was performed: the specimens were heated at a rate of 10 °C/min from 0 to 260 °C and held for 10 min to melt the residual crystals and remove the thermomechanical history, then, they were cooled to 0 °C and re-heated to 260 °C at the same scan rate.

Dynamic-mechanical analysis was carried out using a DMA V4.2C PL analyzer. DMA spectra were recorded in the tensile mode, with an oscillation amplitude of 1 mm, a frequency of 1 Hz and a heating rate of 5 °C/min in the range of $-50 \div 250$ °C.

### 2.4. Results and discussion

The determination of silicate content in ADS copolyamide-based hybrids was performed by gravimetric measurements to ensure an accurate assessment of the level of silicate in each extruded blend. The average values of measured silicate loading with their standard deviations are reported for each specimen and compared to nominal loading in Table 2. Analyzing the results, it can be observed that the differences between the nominal and the measured silicate level are less than 6%, indicating that the melt compounding in our processing conditions has guaranteed a satisfactory control of silicate content in the hybrids.

In order to verify that the Cloisite 30B was dispersed on a nanometric scale in melt compounded samples, TEM and XRD analyses were carried out on hybrid systems and neat copolyamide. In particular, the state of exfoliation and intercalation of silicate platelets inside polymer matrix was investigated by TEM analyses whereas information about the phase structure (in terms of crystalline morphology of polymer matrix, orientation of silicate layers and polymer matrix) of nanocomposite samples was obtained by X-ray analyses.

Table 2
Nominal and measured silicate loading in ADS-based nanocomposites

| Nominal wt% of Cloisite 30B in ADS-based hybrids | Measured wt% of Cloisite 30B $\pm \sigma$ in ADS-based hybrids |
|---|---|
| 3 | $3.1 \pm 0.2$ |
| 6 | $5.9 \pm 0.4$ |
| 9 | $9.3 \pm 0.4$ |

TEM images of hybrids with different clay amount were taken on sections located normal to the extrusion direction, as shown in Fig. 2. The micrographs were captured with different magnification levels on the same normal section of the samples, in order to evidence the hierarchical structure of the hybrids. The low-magnification images show the micron scale arrangement of primary clay particles in the ADS matrix. Higher magnifications reveal a nano-scale dispersed morphology containing both individual silicate sheets and intercalated structures resulting from an extensive penetration of ADS matrix between the organo-clay layers of Cloisite 30B. Transmission electron micrograph of normal sections of 3ADS100, 6ADS100 and 9ADS100 were compared in Figs. 3, 4(a–b) and 5(a–c), respectively.

The figures show that all hybrids are characterized by intercalated/exfoliated morphology, but the degree of exfoliation observed markedly feels the effects of system composition. In fact, the image corresponding to the 3ADS100 nanocomposite (Fig. 3) clearly evidences that the silicate particles are distributed not uniformly in the polymer matrix: micron-scale morphology is comprised of dispersed primary particles and intercalated aggregates surrounded by a distribution of uncorrelated layers. Similar morphology is exhibited by 6ADS100 hybrid (Fig. 4(a–b)), but in this case the aggregates have smaller size, with stack dimensions in the range of 3–10 nm. The layer distribution is not uniform: this result may be associated both to mixing conditions and inhomogeneities (size and composition) inherent in natural montmorillonite that imply a mesoscopic superstructure consisting of compositional fluctuations in the hybrids [4,10]. Figs. 3 and 4(a–b) evidence also that silicate layers are flexible and only locally aligned relative to processing history. On the other hand, the TEM

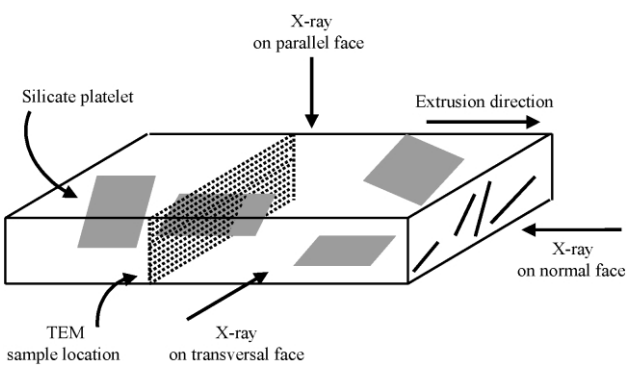


Fig. 2. Schematic representation of incident X-ray paths and TEM sampling location.


Fig. 3. TEM micrograph of normal section of 3ADS100 hybrid.

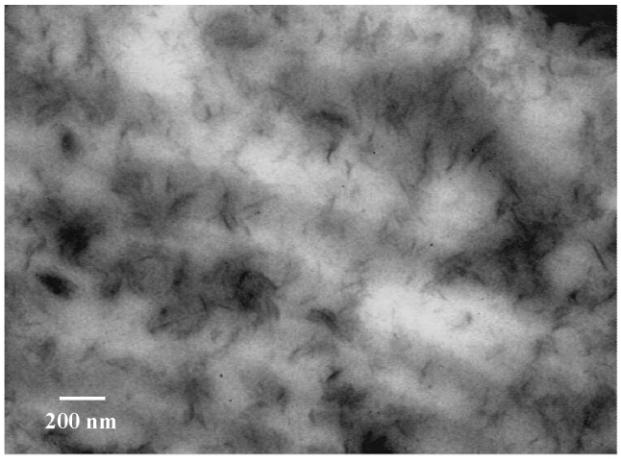


(a)

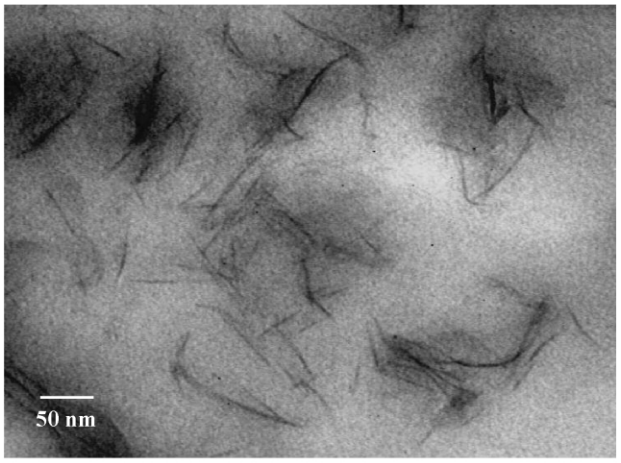


(b)

Fig. 4. TEM micrographs of normal section of 6ADS100 hybrid increasing the magnification levels from (a) to (b).

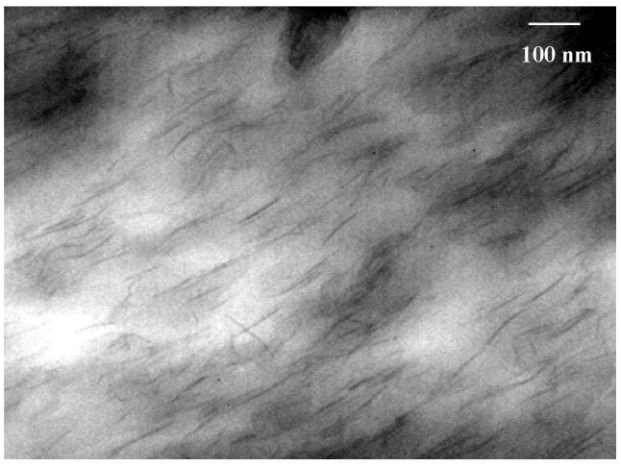


(a)

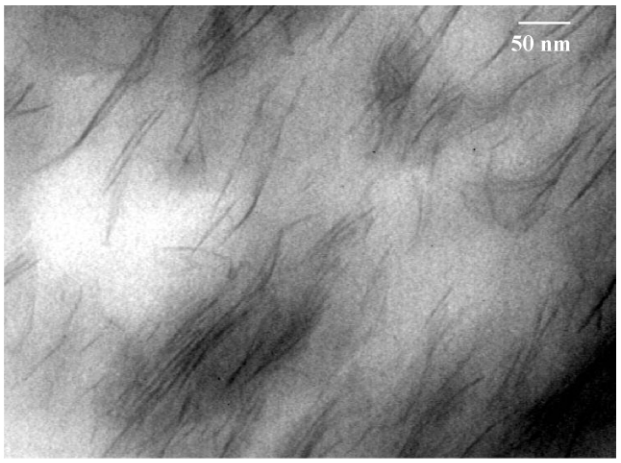


(b)

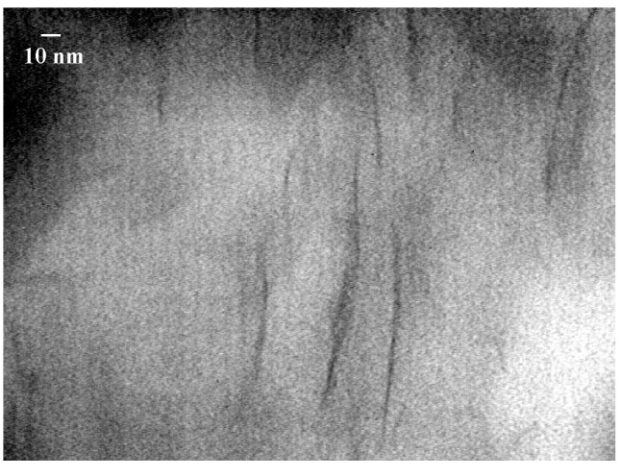


(c)

Fig. 5. TEM micrographs of normal sections of 9ADS100 hybrid increasing the magnification levels from (a) to (c).

micrographs of 9ADS100 (Fig. 5(a–c)) show a significant change in the hybrid morphology: a more homogeneous dispersion of clay particles on micron-scale, with small stack dimensions included in the range of 1–5 nm, and a higher extent of silicate exfoliation on nano-scale with a macroscopic preferential orientation of the layers can be observed at all magnification levels. In particular, the montmorillonite sheet sections appear predominantly parallel to the ribbon plane. This last result is a consequence of both the large anisotropy of the silicate platelets and the shear flow associated with the extrusion process. In fact, it should be considered that a fraction of polymer chains is associated chemically or hydrogen-bonded to the clay surface and, because of the shear, the polymer chains stretched by shear may remain oriented and clay platelets can be aligned in the flow direction. Similar macroscopic layer alignment was already reported in literature for other melt compounded nanocomposite systems [4,12–14, 21–23].

Being all the three hybrids extruded in the same processing conditions, their morphological differences have to be based on concentration of Cloisite 30B. In fact, it has to be noticed that: (1) the chemical and physical polymer–clay interactions determine an increase in the polymer relaxation times and (2) the number of such interactions increases with the silicate amount. This implies that a higher degree of orientation for both clay platelets and polymer chains can be produced by shear in the hybrids with higher silicate loadings [10,13,23].

In order to evidence the extrusion rate effect on the morphology of the hybrids, TEM measurements were also taken on normal sections of nanocomposites melt compounded at 50 rpm. As example, Fig. 6 shows a micrograph of 9ADS50 sample. The image evidences that this hybrid exhibits a bigger stack size and a less homogeneous silicate layers distribution, compared to the 9ADS100 nanocomposite, pointing out that high levels of shear stress aid in the breakup of clay particles and improve clay platelet exfoliation and alignment with the flow.

The state of exfoliation and intercalation inferred from TEM micrographs was further confirmed by XRD analyses, performed both on all melt compounded samples and pristine Cloisite 30B. The measurements were performed on samples oriented normal, transversal and parallel to the extrusion direction, in order to evidence possible orientation phenomena of silicate platelets and matrix. Because the normal and transversal XRD patterns are identical, in the following we refer to the diffractograms obtained on normal face, only. Fig. 7 compares the XRD profiles of neat organoclay and 9ADS100, chosen for its higher exfoliation level, as resulted from TEM investigation. As expected, the Cloisite 30B spectrum shows a peak centered at about $2\theta = 5.2°$ corresponding to a $d$-spacing of 18.5 Å. Analyzing the XRD profile of 9ADS100 hybrid, it clearly appears that the original peak of silicate was shifted to small angle ($2\theta <$ 1°), assuring that the $d$-spacing is become not less than 100 Å, and only a broad shallow peak can be noticed in the $2\theta$ region where the neat organoclay diffracts. These results indicate that the Cloisite 30B is dispersed on a nano-scale in the ADS, confirming TEM analyses. The same indications are obtained analyzing all other ADS based hybrids produced with different clay content and processing conditions. X-ray measurements, in fact, cannot always discriminate between disordered intercalate, partially exfoliated and fully exfoliated morphologies [4].

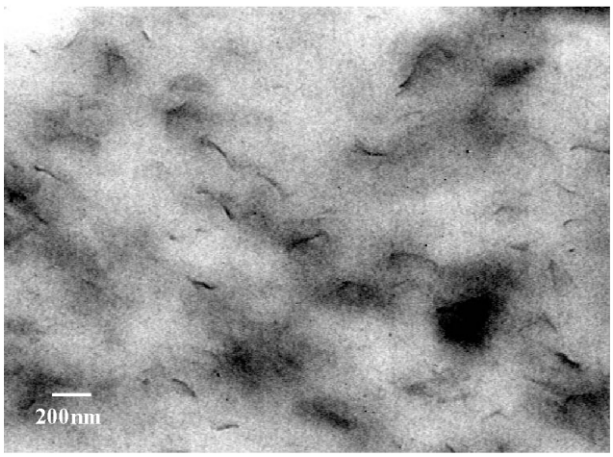


Fig. 6. TEM micrographs of normal section of 9ADS50 hybrid.

The X-ray spectrum of 9ADS100 reported Fig. 7 shows also an intense reflection, centered at $2\theta \sim 11.0°$, and a complex peak with three maxims centered at about 19.5°, 21.2° and 22.5°. The reflections at 19.5° and 22.5° correspond to the α-crystal line phase of the polymer matrix, whereas the two others are associated to the γ-crystalline phase [12]. Similar diffractogram was also obtained for neat copolyamide sample. It is well known, in fact, that polyamides can display polymorphism [24–25]: the α-phase is characterized by extended-chain sheet structure in which adjacent folded anti-parallel chains are

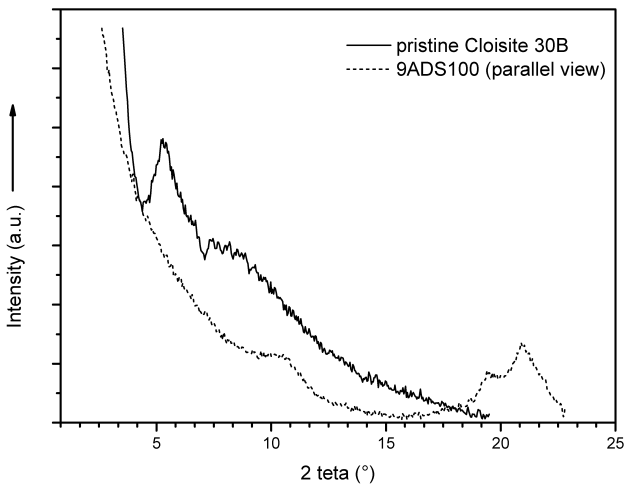


Fig. 7. Comparison of the XRD profiles of pristine organoclay and 9ADS100 hybrid (parallel view).

joined by hydrogen bonds, while the γ phase is composed of plated sheets of twisted parallel chains joined by hydrogen bonds. The α phase is generally dominant being thermodynamically the most stable crystalline form, but the γ phase can be easily obtained under non-isothermal crystallization conditions. Some studies about γ → α crystalline transition of nylon 6-nanocomposites prior to melting [21, 26–31] have demonstrated that the presence of silicate layers affects the phase structure of hybrid systems stabilizing a dominant γ-crystal phase. This stabilizing effect of silicate has been attributed to the polymer-aluminosilicate interactions: the layers affect the amount and the type of crystalline phase because they restrict the mobility of the molecular chains due to both strongly confined spaces between layers and chemical bonds with the clay surface. On the basis of these results it appears of great interest to deepen the investigation of both the morphological behavior of our new copolyamide nanocomposites and the silicate platelets influence on crystal structure and molecular orientation of ADS chains, through more extensive XRD and DSC analyses. In particular, to better evidence orientation phenomena of copolyamide matrix and silicate, the XRD spectra were registered on samples located both normal and parallel to the extrusion direction. At this regard, XRD patterns for 9ADS100 hybrid were taken in parallel and normal face direction and reported in Fig. 8. Comparing the patterns, it can be observed that in the parallel view all diffraction signals are randomly oriented, whereas in the normal view the diffraction signals of both silicate and ADS display a preferred equatorial direction, indicating that both clay platelets and polymer matrix crystallites are aligned in the extrusion direction, confirming TEM analysis. The patterns of Fig. 8 show also a clear coexistence in the ADS matrix of two crystalline forms, α and γ. The stabilizing effect of silicate platelets for the γ crystalline form in ADS-based nanocomposite samples was confirmed annealing at 200 °C for 1 hr both neat ADS matrix and 9ADS100 sample and recording their XRD spectra in parallel and normal views. The obtained diffractograms were reported in Fig. 9(a and b). The X-ray patterns of the annealed samples clearly show that only the

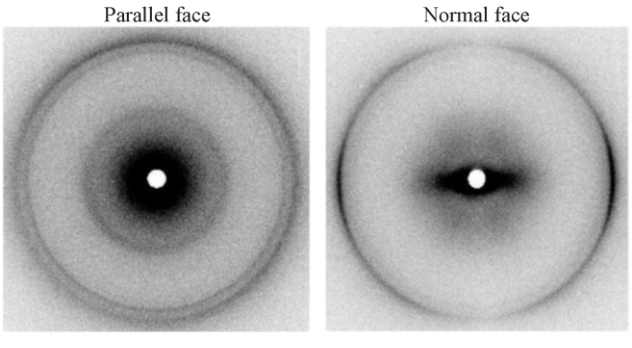


Fig. 8. XRD patterns of 9ADS100 hybrid: (a) parallel view; (b) normal view.

α form with almost no orientation is present in the ADS matrix after the thermal treatment (Fig. 9(a)): the result is a consequence of the crystal-crystal transition (called the *Brill transition* [25]) occurring during the annealing process at 200 °C. Instead, the co-existence of both α and γ crystalline forms, oriented in the extrusion direction, is evident in the annealed hybrid (Fig. 9(b)). This result points out that the presence of silicate in the copolyamide matrix affects on molecular orientation of polymer chains and stabilizes the γ-form, reducing the extent of the Brill transition respect to the neat ADS. Nevertheless, annealing the hybrid for almost 5 h, predominating α form crystalline peaks were observed in the XRD pattern (Fig. 10), similarly to what relieved for the annealed matrix, also if a residual orientation still remains in 9ADS100 sample. Therefore, we can conclude that the addition of Cloisite 30B does not change the relative thermodynamic stability of the two crystalline habits, but reduces the polymer chain mobility as a consequence of the strong polymer–silicate interactions due to the nanometric dispersion of clay platelets in the copolyamide matrix [30].

In order to deepen the influence of nano-scale dispersion of silicate platelets on the phase structure of melt compounded samples, dynamic DSC experiments were carried out on hybrids produced with different extrusion rate and clay content. All nanocomposites were submitted to a thermal cycle described in the Experimental section to erase the thermo-mechanical history of the melt compounded samples. The cooling and second heating DSC traces of

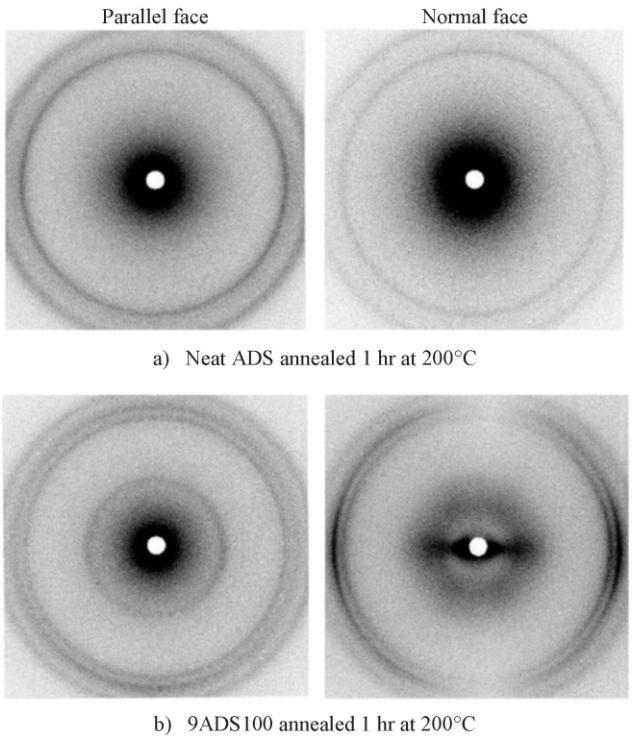


Fig. 9. XRD patterns of samples after annealing at 200 °C for 1 hr: (a) parallel and normal view of neat ADS matrix; (b) parallel and normal view of 9ADS100 hybrid.

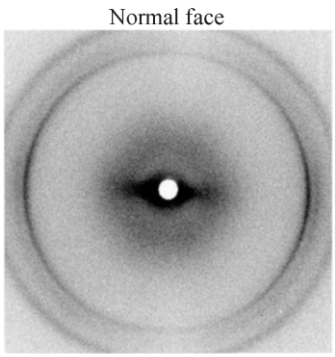


Fig. 10. XRD pattern of 9ADS100 hybrid after annealing at 200 °C for 5 hr (normal view).

ADS matrix and nanocomposite samples are compared in Figs. 11 and 12(a and b), respectively.

Cooling DSC scans have allowed comparing non-isothermal crystallization of neat ADS matrix and all nanocomposite systems. All the thermograms show only one endothermic peak, but some differences in the peak temperatures can be relieved. As example, Fig. 11 shows the DSC cooling traces of neat ADS and 9ADS100 hybrid. The graph evidences that the crystallization peak of the nanocomposite sample is shifted towards slightly lower $T_c$ values. The peak and onset temperature of DSC cooling scans of ADS matrix and all ADS nanocomposites are reported in Table 3. Similar results were already reported in literature on polyamide 6-based nanocomposites [26].

Analyzing the second heating DSC traces (Fig. 12(a and b)), it clearly results that neat ADS thermogram exhibits a complex endothermic melting peak with a maximum centered at about 215 °C and a small shoulder at about $T =$ 207 °C. This thermal response is a consequence of the ADS polymorphism: the lower temperature endotherm can be associated to melting of γ-phase crystallites whereas the higher one to melting of α-phase crystallites, in analogy

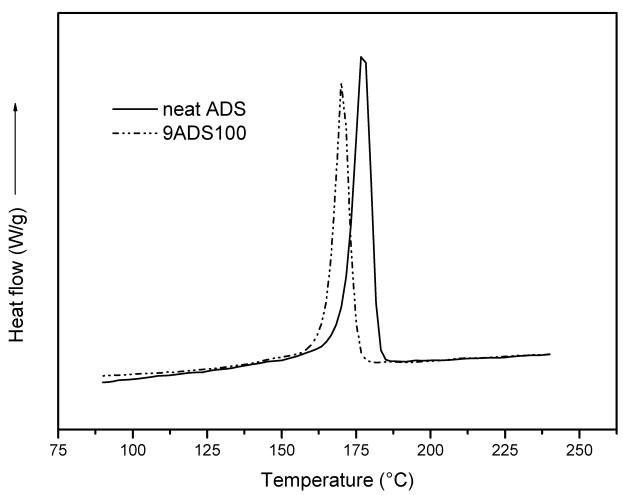


Fig. 11. Cooling DSC thermograms of neat ADS matrix and 9ADS100 hybrid.

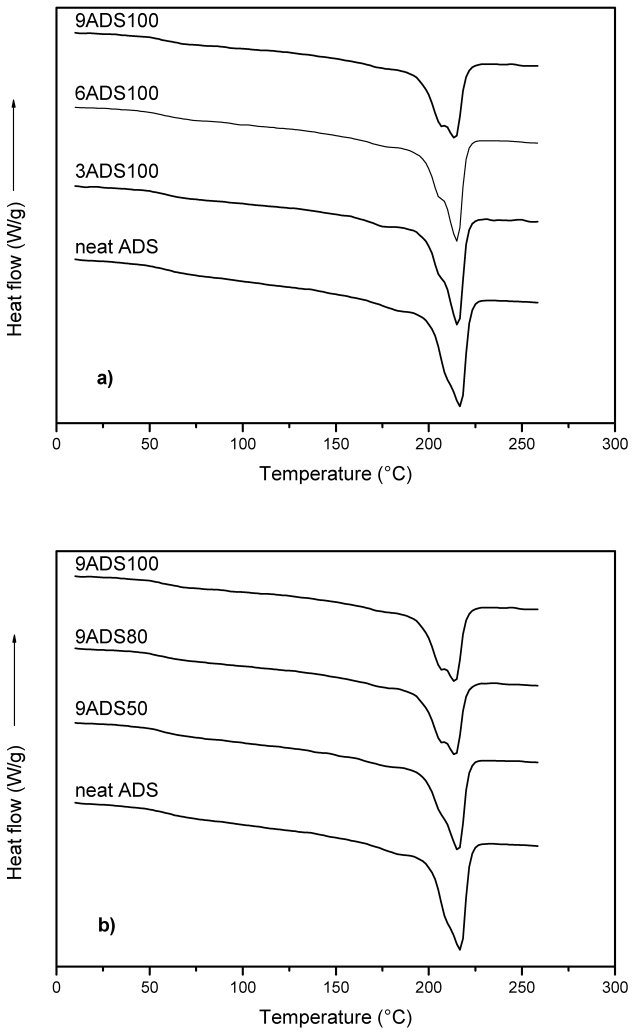


Fig. 12. Second heating DSC thermograms of ADS matrix and nanocomposite samples: (a) effect of silicate loading on hybrids extruded at 100 rpm; (b) effect of extrusion rate on hybrids with 9 wt% of clay.

with what reported in literature for thermal response of polyamide 6 [26–31]. Comparing the DSC traces in Fig. 12(a) it can be also noticed that, increasing the silicate loading, the lower temperature peak becomes more evident respect to the main melting peak. This observation is in

Table 3
Peak and onset temperature of DSC cooling scans of ADS matrix and ADS nanocomposites

| Sample | $T_c$ (°C) | $T_{onset}$ (°C) |
|---|---|---|
| Neat ADS | 181 | 184 |
| 3ADS50 | 176 | 179 |
| 6ADS50 | 172 | 175 |
| 9ADS50 | 174 | 177 |
| 3ADS80 | 176 | 178 |
| 6ADS80 | 172 | 175 |
| 9ADS80 | 171 | 175 |
| 3ADS100 | 175 | 178 |
| 6ADS100 | 171 | 174 |
| 9ADS100 | 170 | 173 |

agreement with the kinetically favored crystallization of ADS into γ-form induced clay, according to X-ray results. Even though the proportion of the γ phase increases with the clay loading, no significant changes are measured in terms of crystallinity degree of ADS matrix, since the melting enthalpy values of the polymer remain almost constant.

Similar trend can be observed comparing the thermograms corresponding to hybrids having the same silicate loading and produced using different extrusion rates. As example, Fig. 12(b) shows the second DSC scans of nanocomposites with 9 wt% of clay, extruded at 50, 80 and 100 rpm: the thermal response of these hybrids, in fact, feels more strongly the effect of processing conditions respect to the systems with lower silicate amount. Since the stabilization of γ-form crystals seems to be a consequence of the strong polymer–clay platelets interactions, the thermal responses compared in Fig. 12(b) suggest that a higher degree of clay dispersion and/or exfoliation in the copolyamide matrix is achieved in the hybrids extruded with higher extrusion rate. At this regard it is worthy to note that several theoretical and experimental studies have demonstrated that a sufficient stress able to shear the silicate particles into small platelets stacks must be provided during the processing to obtain a satisfactory exfoliation degree in melt compounded polymer–silicate systems [4,10–11]. The hypothesis that a more exfoliated morphology is obtained in hybrids extruded with higher extrusion rate was confirmed by rheological investigations performed on these systems and whose results will be reported in a separate paper.

With the aim to further confirm the stabilizing effect of Cloisite 30B on the γ-crystal phase of ADS copolyamide, DSC measurements were also carried out on ADS matrix and 9ADS100 nanocomposite annealed in the same conditions used for XRD analyses (1 and 5 h at 200 °C). The thermal responses obtained from the heating scan performed after annealing were reported in Fig. 13. The graph clearly evidences that the γ-form crystal melting peak disappears in the DSC trace corresponding to neat ADS whereas becomes higher and sharper in the DSC trace corresponding to the 9ADS100 hybrid annealed for 1 h. Nevertheless, after 5 h of thermal annealing, also the nanocomposite system undergoes to Brill transition from the γ to the α crystal form, causing the disappearance of the low temperature melting peak.

All DSC measurements suggest that ADS copolyamide interacts strongly with Cloisite 30B favoring the γ-phase, as concluded also from X-ray investigations, and point out that the increase in either extrusion rate or clay loading of the hybrids may exert an equivalent action on the morphology of melt compounded nanocomposites, as a consequence also of the chosen processing conditions.

Dynamic-mechanical analyses (DMA) have been performed to track the temperature dependence of dynamic storage ($E'$) and loss ($E''$) modulus of the hybrids and to

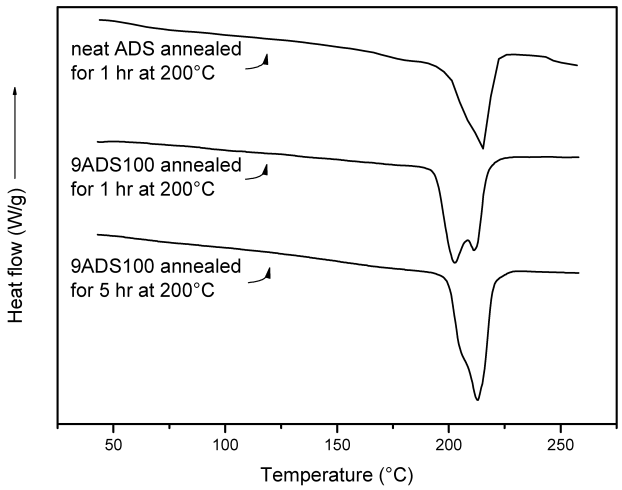


Fig. 13. First heating DSC thermograms of neat ADS and 9ADS100 samples annealed at 200 °C.

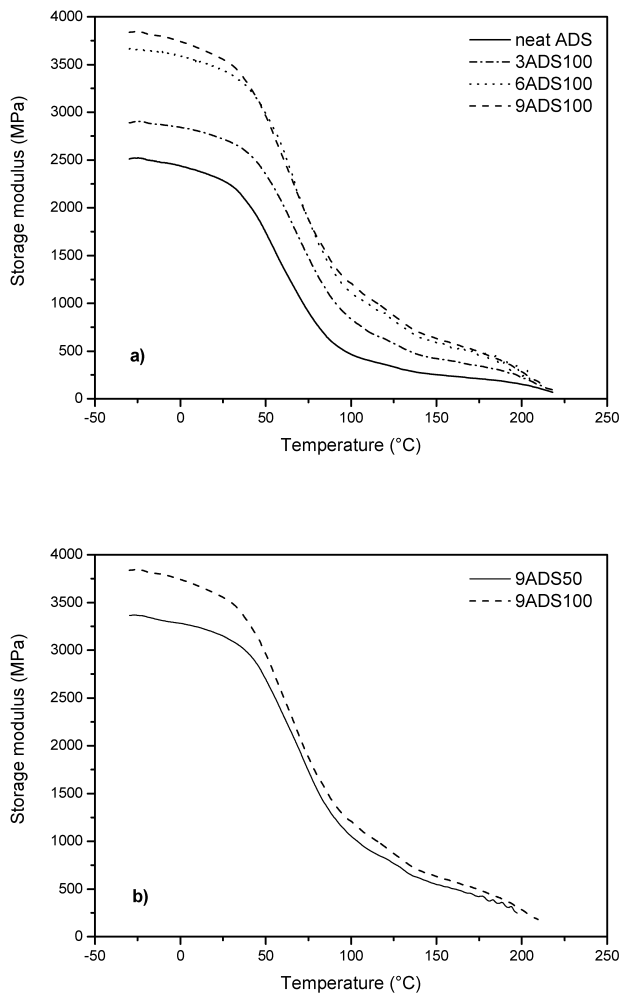


Fig. 14. Storage modulus curves of ADS nanocomposites: (a) samples extruded at 100 rpm with different silicate loadings; (b) samples with 9 wt% of clay extruded at 50 and 100 rpm.

evaluate the influence of clay content on the glass transition. The obtained results are reported in Figs. 14(a and b) and 15.

Fig. 14(a) shows the storage modulus E′ vs. temperature for ADS nanocomposites extruded at 100 rpm with different silicate loadings. The graph clearly points out that the addition of clay into ADS matrix results in a remarkable increase of copolyamide stiffness. The greater the amount of silicate in the hybrid, the more significant is the effect. The increase in E′ values is particularly relevant at lower temperatures, but even in the rubbery plateau the curves of nanocomposite samples are two times or higher than that of pure ADS, indicating that the addition of clay induces a significant reinforcement effect, enhancing the thermal–mechanical stability of the material at high temperatures.

Fig. 14(b) evidences effect of the extrusion rate on the dynamic mechanical response of ADS hybrids with 9 wt% of Cloisite 30B extruded at 50 and 100 rpm. As a consequence of the higher exfoliation degree realized at 100 rpm, the 9ADS100 sample exhibits higher storage modulus in the entire temperature range investigated with respect to the one extruded at 50 rpm.

Fig. 15 shows the loss modulus curves of hybrids extruded at 100 rpm with different clay amounts. It can be noted that the silicate nano-scale dispersion affects enough the glass transition temperature ($T_g$) of the hybrids. In fact, the main peak associated with the glass-rubber transition of the polyamide, appearing at ca. 60 °C in the pure ADS 40T, is shifted towards higher temperature (ca. 70 °C) in nanocomposite systems, even at the lowest clay percentage used (3 wt%). On the other hand, for fixed clay amount the increase in the extrusion rate does not induce significant variations in T-position of E″ peak. The influence of clay on glass transition may be attributed to a soft cross-linking of the hybrid system due to both the confinement of copolyamide matrix in silicate galleries that partially hinders molecular motions and the chemical bonds between the polymer and silicate layers [4,32].

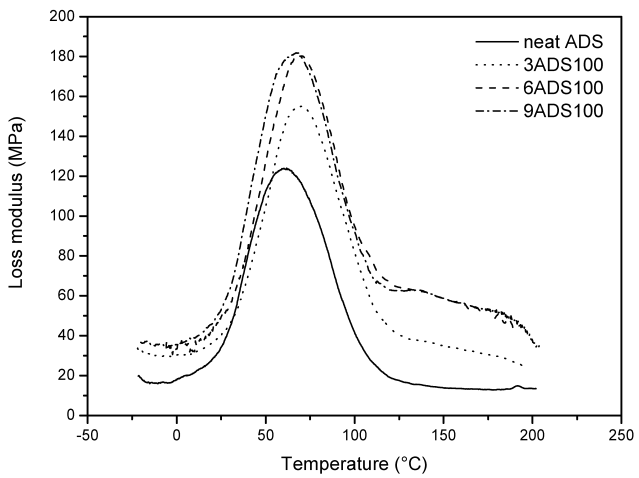


Fig. 15. Loss modulus curves of hybrids extruded at 100 rpm with different clay amounts.

### 2.5. Conclusions

In this study, a new nanocomposite system prepared by melt compounding of a commercial copolymer of polyamide 6 with organically modified montmorillonite was investigated. Hybrids with different silicate loadings extruded at different screw speeds were produced using a twin-screw extruder and characterized in order to establish processing-morphology-property relationships. TEM analyses have shown that all samples exhibit a mixed nanometric dispersion of the silicate, having regions of intercalated and exfoliated clay platelets. However, as increasing of both silicate loading and extrusion rate of the hybrids more and more exfoliated zones and a significant orientation of silicate platelets were observed from TEM and X-ray analyses. The diffractograms have also pointed out that the presence of silicate layers stabilizes the γ-crystalline phase and promotes the molecular orientation of polymer chains as a consequence of copolyamide-silicate sheets interactions that increase the relaxation time of the polymer, favoring its orientation in the flow direction. The X-ray patterns of the annealed samples clearly show that only the α form with almost no orientation is present in the ADS matrix while the co-existence of both α and γ crystalline forms, oriented in the extrusion direction, is evident in the hybrids. The effect of the increasing of extrusion rate and clay loading on the morphology of the hybrids has been shown by thermal analysis in which an equivalent action on stabilizing γ-crystal phase has been observed. Finally, dynamic-mechanical tests have pointed out a remarkable increase of copolyamide stiffness and an enhancement of glass transition temperature with the addition of clay. A similar trend was observed as increasing of the extrusion rate. From the obtained results we can conclude that strong polymer–silicate interactions are present in ADS-based nanocomposites. Moreover, such a copolyamide matrix also shows improved processability, allowing the melt compounding temperatures to be reduced, due to its lower melting point with respect to polyamide 6 homopolymer.

## Acknowledgements

This work was supported by PRIN Project 2001 (Title: Processability and film production of polymer–silicate nanocomposites by melt compounding).

## References

[1] Osborn KR, Jenkins WA. Plastic Films: Technology and Packaging Applications. Lancaster: Technomic Publishing Company, Inc; 1992.

[2] Zilberman M, Siegman A, Narkis M. Polymer 1995;36:5065–7.
[3] Siciliano A, Severgnini D, Seves A, Pedrelli T, Vicini L. J Appl Polym Sci 1996;60:1757–64.
[4] Pinnavaia TJ, Beall GW, editors. Polymer-Layered Silicate Nanocomposites. New York: Wiley; 2001.
[5] Alexandre M, Dubois P. Mater Sci Eng 2000;28:1–63.
[6] LeBaron PC, Wang Z, Pinnavaia TJ. Appl Clay Sci 1999;15:11–29.
[7] Holmes M. Plast Add Comp 2000;7/8:34–6.
[8] Messersmith PB, Giannelis EP. J Polym Sci Part A: Polym Chem 1995;33:1047.
[9] Burnside SD, Giannelis EP. Chem Mater 1994;6:2216.
[10] Cho JW, Paul DR. Polymer 2001;42:1083–94.
[11] Fornes TD, Yoon PJ, Keskkula H, Paul DR. Polymer 2001;42:9929–40.
[12] Varlot K, Reynaud E, Kloppfer MH, Vigier G. J Polym Sci Part B: Polym Phys 2001;39:1360–70.
[13] Medellin-Rodriguez FJ, Burger C, Hsiao BS, Chu B, Vaia R, Phillips S. Polymer 2001;42:9015–23.
[14] Bafna A, Beaucage G, Mirabella F, Mehta S. Polymer 2003;44:1103.
[15] Dennis HR, Hunter DL, Chang D, Kim S, White JL, Cho JW, Paul DR. Polymer 2001;42:9513–22.
[16] Liu L, Qi Z, Zhu X. J Appl Polym Sci 1999;71:1133.
[17] Liu X, Wu Q. Macromol Mater Eng 2002;287:180–6.
[18] Scarfato P, Di Maio L, Incarnato L, Acierno D, Mariano A. Packag Techn Sci 2002;15(1):9–16.
[19] Kubota H, Nowell JB. J Appl Polym Sci 1975;19:1521–38.
[20] Khanna YP, Han PK. Polym Eng Sci 1996;36:1745.
[21] Kojima Y, Usuki A, Kawasumi M, Okada A, Kurauchi T, Kamigaito O, Kaji K. J Polym Sci Part B: Polym Phys 1994;32:625–30.
[22] Morgan A, Gilman JW. J Appl Polym Sci 2003;87:1329–38.
[23] Ranade A, D'Souza NA, Gnade B. Polymer 2002;43:3759–66.
[24] Miyasaka K, Ishikawa K. J Polym Sci 1968;A-2(6):1317.
[25] Murthy NS, Curran SA, Aharoni SM, Minor H. Macromolecules 1991;24:3215.
[26] Wu T-M, Liao C-S. Macromol Chem Phys 2000;201:2820–5.
[27] Wu T-M, Chen E-C, Liao C-S. Polym Eng Sci 2002;42:1141–50.
[28] Devaux E, Boubigot S, Achari A. J Appl Polym Sci 2002;86:2416–23.
[29] Liu X, Wu Q. Eur Polym J 2002;38:1383–9.
[30] Liu X, Wu Q. Polymer 2002;43:1933–6.
[31] Liu X, Wu Q, Berglund LA, Qi Z. Macromol Mater Eng 2002;287:515–22.
[32] McNally T, Raymond Murphy W, Lew CY, Turner RJ, Brennan GP. Polymer 2003;44:2761–72.